

Transport of biomolecules in asymmetric nanofilter arrays

Zi Rui Li · G. R. Liu · Jongyoon Han · Yu Zong Chen ·
Jian-Sheng Wang · Nicolas G. Hadjiconstantinou

Received: 27 August 2008 / Revised: 30 November 2008 / Accepted: 1 December 2008 / Published online: 7 January 2009
© Springer-Verlag 2008

Abstract We propose a theoretical model for describing the electric-field-driven migration of rod-like biomolecules in nanofilters comprising a periodic array of shallow passages connecting deep wells. The electrophoretic migra-

tion of the biomolecules is modeled as transport of point-sized Brownian particles, with the orientational degree of freedom captured by an entropy term. Using appropriate projections, the formulation dimensionality is reduced to one physical dimension, requiring minimal computation and making it ideal for device design and optimization. Our formulation is used to assess the effect of slanted well walls on the energy landscape and resulting molecule mobility. Using this approach, we show that asymmetry in the well shape, such as a well with one slanted and one vertical wall, may be used for separation using low-frequency alternating-current fields because the mobility of a biomolecule is different in the two directions of travel. Our results show that, compared to methods using direct-current fields, the proposed method remains effective at higher field strengths and can achieve comparable separation using a significantly shorter device.

Z. R. Li (✉) · G. R. Liu · Y. Z. Chen · J.-S. Wang
The Singapore-MIT Alliance,
4 Engineering Drive 3,
Singapore 117576, Singapore
e-mail: smalzr@nus.edu.sg

G. R. Liu
Centre for ACES, Department of Mechanical Engineering,
National University of Singapore,
9 Engineering Drive 1,
Singapore 117576, Singapore

J. Han (✉)
Department of Electrical Engineering and Computer Science,
Massachusetts Institute of Technology,
Cambridge, MA 02139, USA
e-mail: jyhan@mit.edu

J. Han
Department of Biological Engineering,
Massachusetts Institute of Technology,
Cambridge, MA 02139, USA

Y. Z. Chen
Department of Pharmacy, National University of Singapore,
6 Science Drive 2,
Singapore 117546, Singapore

J.-S. Wang
Department of Physics, National University of Singapore,
2 Science Drive 3,
Singapore 117542, Singapore

N. G. Hadjiconstantinou
Mechanical Engineering Department,
Massachusetts Institute of Technology,
Cambridge, MA 02139, USA

Keywords Nanofluidics · Asymmetric nanofilter ·
Entropy barrier · DNA separation · Brownian ratchet ·
Molecular transport

Introduction

Separation of biological macromolecules is of great interest to modern biomedical science and engineering. Currently, the most widely adopted separation methods, e.g., gel electrophoresis and gel-exclusion chromatography, use conventional polymeric gel materials as sieving media. Despite the widespread use of gel-based methods, much experimental and theoretical effort has been expended in developing alternative technologies due to the difficulties associated with characterizing the disordered nature of the gel matrix and the resulting limitations in experimental accuracy and functionality.

Recently, significant progress has been made in developing gel-free separation devices by using nanoscale periodic structures [1–5]. In addition to their role as molecular sieving devices, regular microfiltration and/or nanofiltration structures also serve as ideal test beds for the study of molecular dynamics and electromigration of polyelectrolytes because the dimension of obstacles and channels can be precisely measured and controlled. For this purpose, Han and his group have used microfabricated filtration devices consisting of periodic arrays of shallow and deep regions to study the migration of various biomolecules including long DNA [6, 7], rod-like short DNA [8, 9], and small proteins [10]. The promise associated with these devices has resulted in a variety of simulation studies, such as Monte Carlo simulations [11], dissipative particle dynamics [12, 13], Brownian dynamics [14], and continuum transport models [15], seeking to gain more insight into the mechanism of molecular transport in such devices. As a result, the effects of channel geometry, field strength, partition function, diffusion coefficient, and electroosmotic flow have been investigated qualitatively from a variety of points of view.

These studies have established that, in the Ogston sieving regime, where the sizes of migrating molecules are smaller than or similar to that of the pore, entropy loss caused by the constraints in the biomolecule's configurational freedom in the shallow regions dominate the mobility difference between various biomolecules. As a result, in the Ogston sieving regime, biomolecules with similar free-resolution mobilities, such as DNA and RNA, travel with different speeds, with smaller molecules traveling faster than bigger ones. On the contrary, in the entropic trapping regime, where the size of polyelectrolytes is much greater than the size of the pore, longer molecules migrate faster than shorter ones, owing to the increased probability that some parts of the longer flexible molecule enter the pore [7].

The operating principle of such nanofluidic filtration systems is based on an energy landscape that is formed by superposition of a driving electrostatic potential and an entropy barrier in the shallow region of the nanofilter array. Here, the gradient of the electric potential energy is determined by the net molecular charges and the external field applied, while the height of energy barriers is determined by the differences between configurational entropies in the shallow and deep regions. The higher the entropy barrier is, the longer a molecule will be trapped in front of the entrance of the shallow region. Separation of molecules of different sizes is therefore achieved based on the difference in the barrier height.

So far, most simulation studies have focused on square wells even though experimentally this geometry is difficult to achieve [8, 9]. It is currently unclear what the effect of

this is on the observed mobility. Additionally, one might wonder what the effect of slanted walls is or what the effect is if the well symmetry is broken. For example, can geometric asymmetry be used to obtain better separation? In this paper, we try to answer these questions by studying the electrophoretic flow of charged biomolecules in the asymmetric nanofilter arrays in the Ogston sieving regime.

A nanochannel with repeated asymmetric nanofilters can be thought of as Brownian ratchet, which is capable of generating a net mass flux under a zero-average dynamic load [16–20]. So far, transport of Brownian particles in ratchets has been usually studied by stochastic simulation methods such as Monte Carlo simulations [19, 21] or by numerical methods that simulate the Langevin dynamics [16, 22–24]. More accurate molecular dynamics simulations have also been reported but only for very small systems [25]. All these methods are computationally expensive, especially since many rounds of execution of the same process are required for obtaining statistically reliable results for macroscopic times.

Here, we propose a model based on the macroscopic transport description to study the migration of molecule in an asymmetric nanofilter featuring a slanted (right) wall and a vertical (left) wall (see Fig. 1). We will show that when the molecule is driven to the right (Fig. 1), the energy barrier associated with entering the shallow region across sloped sidewalls is lower compared to a well with vertical walls. On the other hand, when the molecule is driven to the left, the height of energy barrier is almost unaffected by the slope in right wall of well. As a result, the effective mobility of a molecule when it moves to the right is increased (compared to a well with vertical walls) while its mobility in the opposite direction is almost unchanged. This phenomenon suggests that a separation method using an alternating current (AC) field is possible. In fact, as we

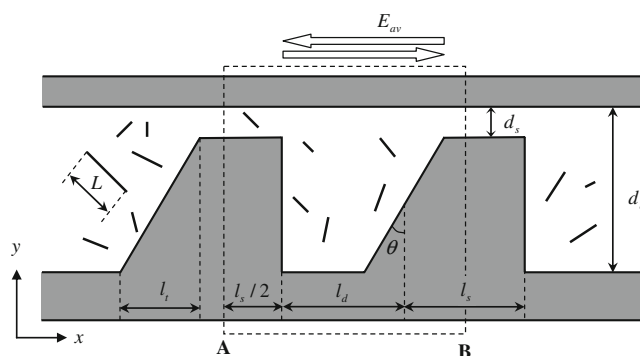


Fig. 1 Structure of the asymmetric nanofilter array. Each unit consists of a right trapezoidal well of maximum depth d_d and a shallow slit of depth d_s . The lengths of the deep region l_d and the shallow region l_s are defined based on the configuration with vertical walls ($\theta=0$), such that their values are not affected by variations in angle θ and the length of transition region (l_t)

show below, it has certain advantages compared to direct current (DC)-field-based methods using a similar geometry that may make it the preferred separation method under certain conditions.

In contrast to Brownian ratchets that utilize the asymmetric potential barrier and the Brownian motion in non-equilibrium state [11], the process described here utilizes the difference in deterministic flux of the molecules when low-frequency external symmetric AC electric fields are applied [26]. The low-frequency field allows the system to reach a quasi-steady state as the molecules are driven to move in one dimension before the direction of the electric field is changed.

As our model is based on a deterministic description of the system, it is easy to implement and is computationally very efficient. Determination of the entropy distribution of a molecule in the discretized channel space (a calculation that needs to be performed only once for every geometry) requires at most a few hours on a normal personal computer, while solving for the mobility of a biomolecule for a given electric field takes only a few minutes. This computational efficiency is very important in the design and optimization of nanofiltration systems, where multiple designs need to be evaluated.

Materials and methods

We model the electrophoretic migration of biomolecules in the nanochannel as a drift-diffusion motion of charged Brownian particles. The effect of configurational degrees of freedom is accounted for using an entropy term that compares the number of permissible microscopic configurational states of a biomolecule in the confined space of the nanochannel to that in the free solution. In addition, since the transport of DNA molecules takes place mainly along the channel axis (*x*-direction), the degree-of-freedom in the depth (*y*-) direction of the channel is eliminated by proper projections. The rationale for such a treatment is fast equilibration in *y*-direction, which is maintained by the translational diffusion that is much faster than the drift speed. In addition, the convective flux induced by the nonuniform electric field at the junction of the deep and shallow regions also helps to establish this equilibrium in *y*-direction in the deep regions.

The above-mentioned simplifications result in a tractable one-dimensional (1D) transport problem, which will be solved using macrotransport theory [27]. More specifically, the 1D energy landscape of the particle will be constructed from the electrostatic potential energy (U_e) and an entropic contribution (U_s). The average migration speed and the effective mobility of the particles will be calculated based on this energy landscape.

Electrostatic potential of a biomolecule in 1D effective nanochannel

The electrophoretic drift of a charged particle with net charge q in an aqueous solution in a static electric field E is balanced by the viscous friction through $qE = \tilde{V}\zeta^e$, where \tilde{V} is the drift speed and ζ^e is the hydrodynamic friction coefficient for electric-driven motion. This phenomenon is usually quantified using the free solution electrophoretic mobility $\mu_0 = \tilde{V}/E = q/\zeta^e$. In addition to field-driven drift, as a consequence of its Brownian motion, the molecule will undergo translational diffusion relative to the surrounding fluid, the magnitude of which is characterized by the translational diffusion coefficient $D = k_B T/\zeta^d$, where k_B is the Boltzmann constant, T is the absolute temperature, and ζ^d is the hydrodynamic friction coefficient for diffusion [28]. For macromolecules such as DNA and proteins, coefficients ζ^e and ζ^d may take different values because the friction to diffusive motion and that to the electric-driven motion are associated with different physical phenomena [29, 30]. In order to unify these diverse phenomena, in the sense that the migration speed of a particle is dependent solely on the gradient of a unified effective potential (an effective force), a unified friction coefficient ($\zeta = \zeta^d$) and a dynamic effective charge $\tilde{q} = k_B T \mu_0 / D$ are adopted. As the values of D and μ_0 are taken from experimental results [31, 32], this effective charge retains the correct electrophoretic mobility ($\mu_0 = \tilde{q}/\zeta^d = q/\zeta^e$), without affecting the description of molecule’s diffusion.

In the geometry considered here, the electric field $E = -\nabla\Phi$ (Φ is the electric potential satisfying $\nabla^2\Phi = 0$) is nonuniform, especially in the deep wells of the nanofilter array. In our projected 1D description, the 1D (projected) potential energy field takes the form

$$U_e(x) = -\tilde{q} \int_0^x E(s) ds, \tag{1}$$

where $E(s)$ denotes the electric field at intra-repeat coordinate s . With reference to Fig. 1, if we define the origin of the local coordinate system of the nanofilter at point A, which denotes the centre of the shallow region with nonslanted channel wall, the electric field in the 1D effective nanofilter can be approximated by

$$E(s) = \begin{cases} \frac{2(1 + \nu_0)}{a_0} E_{av} & 0 \leq s \leq \frac{l_s}{2} \text{ or } \frac{l_s}{2} + l_d + \frac{l_t}{2} < s \leq l_s + l_d \\ \frac{2(1 + \nu_0)\epsilon_0}{a_0} E_{av} & \frac{l_s}{2} < s \leq \frac{l_s}{2} + l_d - \frac{l_t}{2} \\ \frac{2d_d\epsilon_0(1 + \nu_0) \tan \theta}{(\epsilon_0 d_d \tan \theta + s') a_0} E_{av} & \frac{l_s}{2} + l_d - \frac{l_t}{2} < s \leq \frac{l_s}{2} + l_d + \frac{l_t}{2} \end{cases} \tag{2}$$

Here, $l_t = (d_d - d_s) \tan \theta$ is the length of the transition region, E_{av} is the (spatial) average external electric field

given by the total voltage drop over the length of the device, $\varepsilon_0 = d_s/d_d$ ($0 \leq \varepsilon_0 \leq 1$) represents the depth ratio, $\nu_0 = l_s/l_d$ is the length ratio between the shallow and deep region of the nanofilter, and $s' = s - (l_s/2 + l_d - l_t/2)$ denotes the local coordinate for the transition region with sloped channel wall. The dimensionless parameter

$$a_0 = 2(\varepsilon_0 + \nu_0) - (d_d/l_d)(1 + 2\varepsilon_0 \ln \varepsilon_0 - \varepsilon_0^2) \tan \theta \quad (3)$$

accounts for the effect of the slope of the wall.

Entropic barrier in 1D effective channel

The restriction on configurations of a molecule near a solid wall causes a partition of particles according to their distances to the solid walls. As defined here, the local partition function $\kappa(\mathbf{r})$, where $\mathbf{r} \equiv (x, y, z)$ is the position vector of the centre of the molecule, describes the probability of the molecule appearing at \mathbf{r} compared with that in free solution. For a rigid molecule, the configuration is fully described by the molecule's angular orientations (because the diameter of short dsDNA rods is ~ 2 nm, which is very small compared to the length of the molecule and the depth of the channel, the volume exclusion effect is negligible). In this situation, $\kappa(\mathbf{r})$ is equal to the local orientational partition function $\rho_\theta(\mathbf{r})$, which is defined as the ratio of number of permissible orientations to the total number of possible orientations [15, 33]. As we project the 3D nanofilter to 1D channel, the projected partition function $K(x)$ at point x is given by

$$K(x) = \iint_A \kappa(x, y, z) dy dz, \quad (4)$$

where A denotes the cross-section of the nanofilter at point x in the channel axis. Since the local partition function $\kappa(x, y, z)$ characterizes the amount of configurational states of a molecule near channel walls, and the integration domain A determines the number of translational microscopic states accessible to the molecule in the direction perpendicular to x , the partition function $K(x)$ corresponds to an entropic contribution

$$U_s(x) = -k_B T \ln K(x) \quad (5)$$

to the potential energy landscape.

Transport theory

Let $P(X, t)$ denote the 1D probability density function of Brownian particle at point X within the device and time t . The evolution of $P(X, t)$ due to the 1D potential energy landscape $U(X)$ is governed by the Fokker–Planck equation [34],

$$\frac{\partial P(X, t)}{\partial t} = \frac{\partial}{\partial X} J(X, t), \quad (6)$$

with the probability flux given by

$$J(X, t) = -\frac{k_B T}{\varsigma} \frac{\partial P(X, t)}{\partial X} - \frac{1}{\varsigma} P(X, t) \frac{dU(X)}{dX}. \quad (7)$$

The probability density function satisfies the normalization condition

$$\int_{-\infty}^{\infty} P(X, t) dX = 1. \quad (8)$$

According to macrotransport theory [27, 35], the mean velocity of the Brownian particle in a periodic structure can be obtained through the computation of a scalar intra-repeat field $P_0^\infty(x)$, which describes the long-time particle probability density as a function of the local coordinate x , regardless of the specific repeat it resides in. Under this formulation, the reduced probability function $P_0^\infty(x)$ is governed by the conservation law

$$\frac{d}{dx} J_0^\infty(x) = 0 \quad (9)$$

where the probability flux $J_0^\infty(x)$ is given by

$$J_0^\infty(x) = -\frac{k_B T}{\varsigma} \frac{dP_0^\infty(x)}{dx} - \frac{1}{\varsigma} P_0^\infty(x) \frac{dU(x)}{dx}. \quad (10)$$

The periodicity condition requires that $P_0^\infty(x)$ must be continuous at the adjacent repeat of the nanochannel, which means that values of $P_0^\infty(x)$ at two ends of the 1D channel must be equal, i.e.,

$$P_0^\infty(0) = P_0^\infty(l_r). \quad (11)$$

where $l_r = l_s + l_d$ denotes the repeat length of the unit nanofilter.

Also, the normalization condition requires that

$$\int_0^{l_r} P_0^\infty(x) dx = 1. \quad (12)$$

From (9), one knows that $J_0^\infty(x)$ is independent of x , i.e., $J_0^\infty(x) = J_0$. Next, multiplying both sides of (10) by $e^{U(x)/k_B T}$, and integrating the products over one repeat of nanofilter (cf. Fig. 1), the following expression for the probability flux is obtained

$$J_0 = \frac{k_B T}{\varsigma} \left(P_0^\infty(A) e^{U(A)/k_B T} - P_0^\infty(B) e^{U(B)/k_B T} \right) / \int_A^B e^{U(x)/k_B T} dx. \quad (13)$$

Although the explicit expression of $P_0^\infty(x)$ is not available for this problem, it can be solved from (10) and (13) numerically. Once J_0 and $P_0^\infty(x)$ are known, the effective drift velocity of the particle at point x is given by

$$V(x) = J_0 / P_0^\infty(x). \quad (14)$$

The average velocity

$$\bar{V} = \int_0^l J(x) dx = l_r J_0 \tag{15}$$

and the effective mobility over the nanofilter

$$\mu = \bar{V} / E_{av} = l_r J_0 / E_{av} \tag{16}$$

are finally obtained.

Results and discussions

As an example, we study the molecular transport of a 300 bp dsDNA molecule through asymmetric nanofilter arrays as shown in Fig. 1. For simplicity, for calculating the configurational entropy, we treat the molecule as a rigid rod, whose length is given by the Kratky–Porod model [36, 37]. The free-solution mobility $\mu_0 = 3.72 \times 10^{-4} \text{cm}^2 \text{V}^{-1} \text{s}^{-1}$ [32] and free-solution diffusion coefficient $D = 2.07 \times 10^{-7} \text{cm}^2 \text{s}^{-1}$ [31] are adopted from experimentally established data or formula. In the presence of electroosmotic flow, the effective mobility of the molecule is given by $\tilde{\mu}_0 = \mu_0 + \mu_{EEO}$, where μ_{EEO} represents the effective mo-

bility due to electroosmotic flow. This superposition is possible due to the similarity between the profiles of electroosmotic flow and external electric field [38]. Previous simulation work [15] has shown that good agreement with experimental data can be achieved with $\mu_{EEO} = -2.87 \times 10^{-4} \text{cm}^2 \text{V}^{-1} \text{s}^{-1}$.

To investigate the effect of slant angle, we present results for $\theta=0, \pi/12, \pi/6, \text{ and } \pi/4$. The other nanofilter parameters are $d_s=60 \text{ nm}$, $d_d=240 \text{ nm}$, $l_s=l_d=500 \text{ nm}$ (as $\theta=0$).

The entropy landscape is calculated by discretizing the nanofilter using M quadrilateral elements. Local partition functions $\kappa(\mathbf{r}_n)$ ($n=1, \dots, M$) of the DNA molecules are calculated at the centers \mathbf{r}_n of these elements. Assuming that dsDNA molecules are sufficiently short to behave as a rigid rod in aqueous solution, the configuration of these molecules involves only orientational degrees of freedom. Therefore, $\kappa(\mathbf{r}_n)$ can be estimated numerically by enumeration of all the possible orientations of the molecule at \mathbf{r}_n and checking the permissibility of these orientations. The entropy field U_s is then obtained by projecting the 2D field onto a 1D field as explained in “Entropic barrier in 1D effective channel.” The result for U_s for a 300 bp DNA as a function of the slant angle are shown in Fig. 2b. Comparing

Fig. 2 Potential energy landscapes of a 300 bp dsDNA in asymmetric nanofilter channels with different slant angles under the action of an electric field of strength $E_{av}=200 \text{ V/cm}$. **a** The electrostatic potential energy U_e . **b** The entropy landscape U_s . **c** Potential energy landscape $U(x) = U_e(x) + U_s(x)$ when the molecule is driven to the right. **d** The potential energy landscape when the molecule is driven to the left

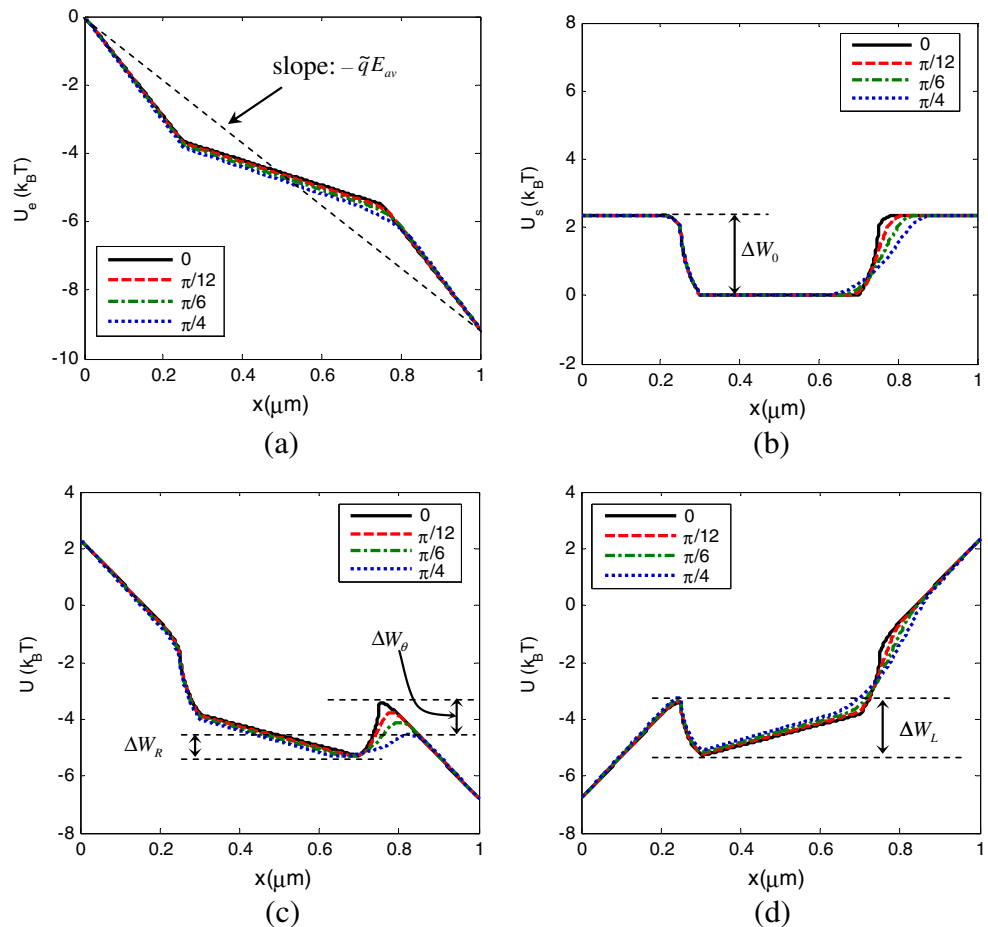
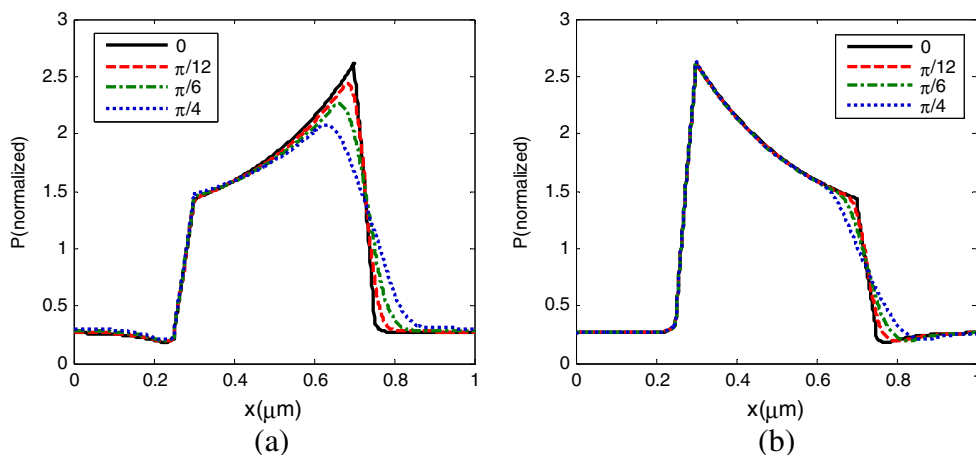


Fig. 3 Intra-repeat probability distribution function $P_0^\infty(x)$ of 300 bp dsDNA in nanofilters with varied slant angles under electric field $E_{av}=200$ V/cm **a** when the molecule moves to the right, and **b** when it moves to the left



with the results of Fig. 2a, which shows the electrostatic potential U_e for $E_{av}=200$ V/cm, it can be seen that the influence of the slant angle on the entropic barrier is much more significant than on the electric potential.

We calculate the potential energy landscape by the superposition of the electric potential and the entropy terms. Figure 2c shows the resulting energy landscape when the molecule is driven to the right, while Fig. 2d shows the energy landscape for a molecule driven to the left. Comparison of these two plots shows that the energy barrier in Fig. 2c is significantly affected by θ in contrast to the energy barrier in Fig. 2d.

From the energy landscapes shown in Fig. 2c and d, we calculate the probability fluxes J_0 and the intra-repeat probability distribution functions $P_0^\infty(x)$ when the DNA molecule moves in the asymmetric nanofilters in the right (forward) and the left (backward) directions. We find that, when driven to the right, the aggregation of molecules in the deep region is significantly decreased as the slant angle changes from 0 to $\pi/4$ (see Fig. 3a). This is because the energy barrier of a molecule in channels with high slant

angle is lower, permitting more molecules to pass the barrier and move to the next repeat. By contrast, when the molecule is driven in the backward direction, the probability distribution curves are almost identical near the vertical wall before the entrance to the shallow region (cf. Fig. 3b), corresponding to similar barrier heights as depicted in Fig. 2d.

Figure 4 shows the relative mobility ($\mu^* = \mu/\mu_0$) of a 300 bp DNA molecule in the asymmetric nanofilters under an $E_{av}=200$ V/cm electric field in both forward and backward directions. We find that the mobility of the molecule in the forward direction is influenced significantly by the slope in the channel wall. Higher slant angle in the channel wall produces a higher effective mobility in the forward direction because the transition rate is determined by the integration of the exponential of the potential energy (cf. (13) and Fig. 2c). By contrast, the mobility of the molecule is much less affected by changes in slant angle when the molecule is driven backward in the same nanochannel.

The difference between mobilities in the forward and backward directions, $\Delta\mu = \mu_{forward} - \mu_{backward}$, which actually represents the net mobility of a molecule under a low-frequency symmetric AC field, can be used to realize molecular separation. (Here, the symmetric AC field is implemented by periodically applying a field with constant magnitude E_{av} for a half period in one direction, then reverse the direction of the field and maintain its strength E_{av} for another half period.) To illustrate this, we calculated the net relative mobilities $\Delta\mu^* = \Delta\mu/\mu_0$ of 50, 150, and 300 bp dsDNA molecules in an asymmetric nanofilter with slant angle $\theta = \pi/4$ under various electric field strengths (see Fig. 5a). We find that using low-frequency AC fields, molecules with higher charge move faster in an asymmetric nanochannel than those with lower charge. In addition, a higher electric field will produce a greater mobility difference. For example, Fig. 5a shows that the difference between the net mobilities of dsDNA molecules is very

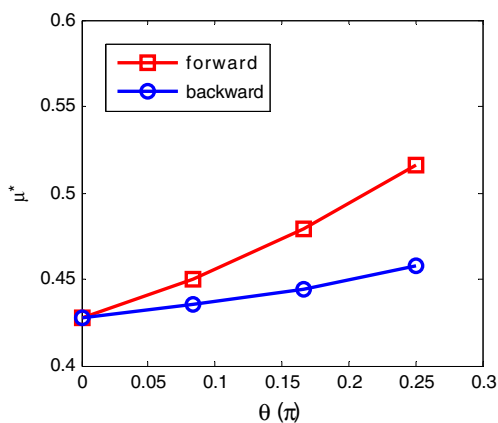
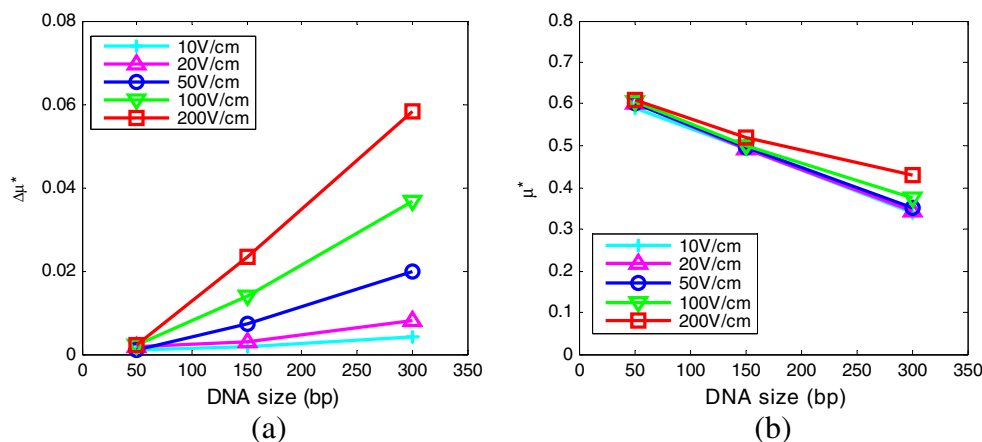


Fig. 4 The relative mobility ($\mu^* = \mu/\mu_0$) as a function of the slant angle. The difference between mobilities in forward and backward directions increases with tilt angle θ

Fig. 5 a The relative net mobility ($\Delta\mu^*$) of dsDNA of different sizes over a nanofilter array with a slant angle of $\theta = \pi/4$ in the channel wall, under symmetric AC fields of varied strengths. **b** The dependence of the relative mobility μ^* of dsDNA over the nanofilter with a vertical wall ($\theta=0$) under different DC fields



small under a low AC electric field of $E_{av}=10$ V/cm. On the other hand, under a stronger AC field ($E_{av}=200$ V/cm), the net mobility of a 300 bp long DNA is about 2.5 times greater than that the mobility of 150 bp long molecule, while the net mobility of 50 bp DNA is almost zero. For comparison purposes, Fig. 5b shows the relative mobility of the same DNA molecules in a nanofilter array with rectangular wells under a DC electric field. This figure shows that, while the DC-field-based method provides a larger difference in mobility between molecules of size 50 and 300 bp, the AC-field-based method requires a much smaller device to achieve comparable performance, especially since the reduction in mobility difference can potentially be recouped using a higher electric field magnitude. This is because, as explained above, higher electric field magnitude results in higher net mobility difference, in contrast to DC-field-based methods, which operate efficiently only under relatively low electric fields. Under higher electric fields, the stronger electric force overcomes the entropic barrier easily and compromises the separation effect [15] (cf. Fig. 5b).

The results in Figs. 4 and 5a may help us to gain some qualitative insights into the differences between the transport mechanisms using AC and DC fields. With reference to Fig. 2, according to Kramers rate theory, $\mu_{forward} \sim e^{-\Delta W_R/k_B T}$ and $\mu_{backward} \sim e^{-\Delta W_L/k_B T}$. From the relationships $\Delta W_\theta = \Delta W_L - \Delta W_R \approx \tilde{q} E_{av} l_t$ and $\Delta W_L \approx \Delta W_0 = -k_B T \ln \varepsilon_0 K$, we obtain the net mobility in an AC field $\Delta\mu \sim (e^{y_t} - 1)\varepsilon_0 K$, where $\varepsilon = d_s/d_d$ is the depth ratio, $K = K_s/K_d$ is the partition coefficient defined as the ratio of average partition functions in shallow (K_s) and deep (K_d) regions, and $y_t = \tilde{q} E_{av} l_t/k_B T$ denotes the dimensionless potential drop in the transition region (with sloped channel wall). This expression for $\Delta\mu$ can be used to provide a qualitative understanding of the dependence of $\Delta\mu$ on various system parameters. In a specific channel with given l_t and ε_0 , $\Delta\mu$ grows exponentially with y_t , which is proportional to the product of field strength E_{av} and the effective charge of the molecule \tilde{q} , the latter of which is

dependent on the length of the molecule (L). In addition, $\Delta\mu$ increases linearly with K , which is also dependent on L (K_s and K_d are functions of L/d_s and L/d_d , respectively [33]). The factors that may produce low mobility in the AC field may include any one or a combination of: (1) low electric field (data for 10 V/cm in Fig. 5a), low charges (50 bp DNA in Fig. 5a), small tilt angle ($\theta \rightarrow 0$, $l_t \rightarrow 0$, see Fig. 4) or extremely low partition coefficient ($K \rightarrow 0$, a trivial condition that permits very few particles to pass through). The system parameters that may produce high mobility in an AC field can be identified in a similar way. The case $y_t \ll 1$, which is valid in most experiments involving short molecules and low-to-medium field, is of particular interest. In this limit, $\Delta\mu$ is approximately proportional to \tilde{q} , E_{av} , and $\tan\theta$ ($\sim\theta$, when θ is small). This explains the (approximately) linear dependence of $\Delta\mu$ on these factors as observed in Figs. 4 and 5a. In contrast, the length dependence of mobility in a DC field as shown in Fig. 5b, where longer molecules possess lower mobilities, is a result of the scaling law $\mu \sim e^{-\Delta W_0/k_B T} \sim \varepsilon_0 K$ in the low-to-medium field regime. Because the partition function K of a longer molecule is smaller than that of a shorter one, its mobility in a DC field is smaller.

The dependence of the net mobility on the field strengths in this paper is in line with that obtained by the molecular dynamics simulation conducted by Chinappi et al. [25], although in [25], the authors dealt with a much smaller system describing the transport of liquid argon atoms across a nanopore with varied diameter from 0.75 to 1.25 nm.

It is not noteworthy that for our model to be accurate, the frequency of AC field in x -direction should be low enough such that the molecules have enough time to pass at least a few repeats before the direction of the field reverses. Otherwise, the quasi-steady state is not established, and the calculated steady-state flux is not reliable. Particularly, if the period of the electric field is shorter than the time for a molecule to move over one period, no deterministic flux should be expected (as observed in [25]), since molecules will not have the opportunity to sample the difference in energy barriers.

Concluding remarks

We proposed a theoretical model that analyzes the electrophoretic motion of biomolecules in nanoscale devices. It was used to assess an asymmetric nanochannel device consisting of a vertical (left) wall and a slanted (right) wall in the well region. We show that the maximum height of the energy barrier is lowered by the wall slope when the molecule is driven towards the slanted wall. In contrast, when driven in the opposite direction, the energy barrier is much less affected. As a result, the mobility of a biomolecule in one direction is greater than that in the reverse direction. Because the mobility difference (in different directions) of a highly charged biomolecule is significantly larger than that of molecules with low charge at medium to high electric fields, we may implement a separation method using low-frequency AC field. The dependence of the mobility on various parameters, such as the strength of external field, the tilt angle at the channel wall, the length and the charge molecule etc., are described using numerical simulations and qualitative arguments. Compared to DC-field-based methods, this method permits higher operating electric fields. It can be expected to produce comparable separation performance while requiring a significantly shorter device. The model requires minimal computation and is thus ideal for device design and optimization.

Acknowledgments This work was funded by Singapore-MIT Alliance (SMA)-II, Computational Engineering (CE) programme. ZR Li wishes to thank former NUS professor N. M. Kochevsky for reading the manuscript and offering most helpful suggestions. ZR Li also thanks Dr. X. Xu (SMA) for helpful discussions on numerical computational methods.

References

- Volkmoth WD, Austin RH (1992) DNA electrophoresis in microlithographic arrays. *Nature* 358:600–602
- Turner SW, Perez AM, Lopez A, Craighead HG (2001) Monolithic nanofluid sieving structures for DNA manipulation. *J Vac Sci Technol B* 16:3835–3840
- Han JY, Fu JP, Schoch RB (2008) Molecular sieving using nanofilters: past, present and future. *Lab Chip* 8:23–33
- Eijkel JCT, van den Berg A (2006) Nanotechnology for membranes, filters and sieves. *Lab Chip* 6:19–23
- Chou CF, Austin RH, Bakajin O, Tegenfeldt JO, Castelino JA, Chan SS, Cox EC, Craighead H, Darnton N, Duke T, Han J, Turner S (2000) Sorting biomolecules with microdevices. *Electrophoresis* 21:81–90
- Han J, Turner SW, Craighead HG (1999) Entropic trapping and escape of long DNA molecules at submicron size constriction. *Phys Rev Lett* 83:1688–1691
- Han J, Craighead HG (2000) Separation of long DNA molecules in a microfabricated entropic trap array. *Science* 288:1026–1029
- Fu J, Yoo J, Han J (2006) Molecular sieving in periodic free-energy landscapes created by patterned nanofilter arrays. *Phys Rev Lett* 97:018103
- Fu J, Schoch RB, Stevens AL, Tannenbaum SR, Han J (2007) A patterned anisotropic nanofluidic sieving structure for continuous-flow separation of DNA and proteins. *Nature Nanotech* 2:121–128
- Fu J, Mao P, Han J (2005) A nanofilter array chip for fast gel-free biomolecule separation. *Appl Phys Lett* 87:263902
- Tessier F, Slater GW (2002) Strategies for the separation of polyelectrolytes based on non-linear dynamics and entropic ratchets in a simple microfluidic device. *Appl Phys A* 75:285–291
- Duong-Hong D, Wang J-S, Liu GR, Chen YZ, Han J, Hadjiconstantinou NG (2008) Dissipative particle dynamics simulations of electroosmotic flow in nano-fluidic devices. *Microfluid Nanofluid* 4:219–225
- Cheng KL, Sheng YJ, Jiang S, Tsao HK (2008) Electrophoretic size separation of particles in a periodically constricted microchannel. *J Chem Phys* 128:101101
- Laachi N, Delet C, Matson C, Dorfman KD (2007) Nonequilibrium transport of rigid macromolecules in periodically constricted geometries. *Phys Rev Lett* 98:098106
- Li ZR, Liu GR, Chen YZ, Wang J-S, Bow H, Cheng Y, Han J (2008) Continuum transport model of Ogston sieving in patterned nanofilter arrays for separation of rod-like biomolecules. *Electrophoresis* 29:329–339
- Reimann P (2002) Brownian motors: noisy transport far from equilibrium. *Phys Rep* 361:57–265
- Leibler S (1994) Brownian motion: moving forward noisily. *Nature* 370:412–413
- Rousselet J, Salome L, Ajdari A, Prost J (1994) Directional motion of Brownian particles induced by a periodic asymmetric potential. *Nature* 370:446–448
- Prost J, Chauwin J-F, Peliti L, Ajdari A (1994) Asymmetric pumping of particles. *Phys Rev Lett* 72:2652–2655
- Astumian RD, Bier M (1994) Fluctuation driven ratchets: molecular motors. *Phys Rev Lett* 72:1766–1769
- Duke TAJ, Austin RH (1998) Microfabricated sieve for the continuous sorting of macromolecules. *Phys Rev Lett* 80:1552–1555
- Reimann P, Hanggi P (2002) Introduction to the physics of Brownian motors. *Appl Phys A* 75:169–178
- Matthias S, Müller F (2003) Asymmetric pores in a silicon membrane acting as massively parallel brownian ratchets. *Nature* 424:53–57
- Reimann P, Evstigneev M (2007) Pulsating potential ratchet. *Europhys Lett* 78:50004
- Chinappi M, de Angelis E, Melchionna S, Casciola CM, Succi S, Piva R (2006) Molecular dynamics simulation of ratchet motion in an asymmetric nanochannel. *Phys Rev Lett* 97:144509
- Derényi I, Astumian RD (1998) AC Separation of particles by biased Brownian motion in a two-dimensional sieve. *Phys Rev E* 58:7781–7784
- Brenner H, Edwards DA (1993) *Macrotransport process*. Butterworth-Heinemann, Boston, MA
- Berg HC (1983) *Random walks in biology*. Princeton University Press, Princeton, New Jersey
- Mercier J-F, Slater GW (2006) Universal interpolating function for the dispersion coefficient of DNA fragments in sieving matrices. *Electrophoresis* 27:1453–1461
- Stellwagen E, Lu YJ, Stellwagen NC (2003) Unified description of electrophoresis and diffusion for DNA and other polyions. *Biochemistry* 42:11745–11750
- Nkodo AE, Garnier JM, Tinland B, Ren H, Desruisseaux C, McCormick LC, Drouin G, Slater GW (2001) Diffusion coefficient of DNA molecules during free solution electrophoresis. *Electrophoresis* 22:2424–2432

32. Stellwagen NC, Gelfi C, Righetti PG (1997) The free solution mobility of DNA. *Biopolymers* 42:687–703
33. Giddings JC, Kucera E, Russell CP, Myers MN (1968) Statistical theory for the equilibrium distribution of rigid molecules in inert porous networks. Exclusion chromatography. *J Phys Chem* 72:4397–4408
34. Ajdari A, Prost J (1991) Free-flow electrophoresis with trapping by a transverse inhomogeneous field. *Proc Natl Acad Sci U S A* 88:4468–4471
35. Yariv E, Dorfman KD (2007) Electrophoretic transport through channels of periodically-varying cross section. *Phys Fluids* 19:037101
36. Kratky O, Porod G (1949) Röntgenuntersuchung gelöster Fadenmoleküle. *Rec Trav Chim Pays-Bas* 68:1106–1123
37. Marko JF, Siggia ED (1995) Stretching DNA. *Macromolecules* 28:8759–8770
38. Cummings EB, Griffiths SK, Nilson RH, Paul PH (2000) Conditions for similitude between the fluid velocity and electric field in electroosmotic flow. *Anal Chem* 72:2526–2532